HHS Public Access

Author manuscript

Environ Sci Technol. Author manuscript; available in PMC 2016 April 07.

Published in final edited form as:

Environ Sci Technol. 2015 April 7; 49(7): 4274–4282. doi:10.1021/es505842v.

Role of Biofilm Roughness and Hydrodynamic Conditions in *Legionella pneumophila* Adhesion to and Detachment from Simulated Drinking Water Biofilms

Yun Shen[†], **Guillermo L. Monroy**[‡], **Nicolas Derlon**[∥], **Dao Janjaroen**[†], **Conghui Huang**[†], **Eberhard Morgenroth**[∥,⊥], **Stephen A. Boppart**[‡,§], **Nicholas J. Ashbolt**[#], **Wen-Tso Liu**[†], and **Thanh H. Nguyen**[†,*]

[†]Department of Civil and Environmental Engineering, University of Illinois at Urbana—Champaign, Urbana, Illinois 61801, United States [‡]Department of Bioengineering, University of Illinois at Urbana—Champaign, Urbana, Illinois 61801, United States [§]Department of Electrical and Computer Engineering, University of Illinois at Urbana—Champaign, Urbana, Illinois 61801, United States [∥]Eawag: Swiss Federal Institute of Aquatic Science and Technology, 8600 Dübendorf, Switzerland [⊥]ETH Zürich, Institute of Environmental Engineering, 8093 Zürich, Switzerland [#]School of Public Health, University of Alberta, Edmonton, Alberta T6G 2G7, Canada

Abstract

Biofilms in drinking water distribution systems (DWDS) could exacerbate the persistence and associated risks of pathogenic *Legionella pneumophila* (*L. pneumophila*), thus raising human health concerns. However, mechanisms controlling adhesion and subsequent detachment of *L. pneumophila* associated with biofilms remain unclear. We determined the connection between *L. pneumophila* adhesion and subsequent detachment with biofilm physical structure characterization using optical coherence tomography (OCT) imaging technique. Analysis of the OCT images of multispecies biofilms grown under low nutrient condition up to 34 weeks revealed the lack of biofilm deformation even when these biofilms were exposed to flow velocity of 0.7 m/s, typical flow for DWDS. *L. pneumophila* adhesion on these biofilm under low flow velocity (0.007 m/s) positively correlated with biofilm roughness due to enlarged biofilm surface area and local flow conditions created by roughness asperities. The preadhered *L. pneumophila* on selected rough and smooth biofilms were found to detach when these biofilms were subjected to higher flow velocity. At the flow velocity of 0.1 and 0.3 m/s, the ratio of detached cell from the smooth biofilm surface was from 1.3 to 1.4 times higher than that from the rough biofilm surface, presumably because of the low shear stress zones near roughness asperities. This study determined that physical structure and local hydrodynamics control adhesion and detachment from simulated drinking water biofilm, thus it is the first step toward reducing the risk of *L. pneumophila* exposure and subsequent infections.

[*]**Corresponding Author**. thn@illinois.edu.

The authors declare no competing financial interest.

INTRODUCTION

Biofilms are ubiquitous in drinking water distribution systems (DWDS). The presence of biofilm potentially increases the persistence and associated risks of pathogens.[1–4] DWDS biofilms provide a favorable environment for capture, growth, propagation, and release of pathogens, such as *Legionella pneumophila* (*L. pneumophila*), by supplying nutrients[5–9] and protecting pathogens from disinfection.[10–12] *L. pneumophila* is known as the main causative agent of legionellosis,[13] which is reported worldwide. In the United States, 3688 legionellosis disease cases were reported in 2012.[14] *L. pneumophila* contributed to 58% of total waterborne disease outbreaks associated with U.S. drinking water between 2009 and 2010.[15] In Europe, 5952 legionellosis disease cases were reported by 29 countries in 2012. The investigation conducted for some of these cases found that water distribution system contributed to 62% of all sampling sites with positive *L. pneumophila* test results.[16] While DWDS biofilms can harbor *L. pneumophila*, the role of biofilms in accumulation and release of *L. pneumophila* is still largely overlooked. Notably, adhesion (capture) of *L. pneumophila* to biofilms is a prerequisite of *L. pneumophila* persistence and propagation, and subsequent detachment (release) of *L. pneumophila* from biofilms under high flow results in the increased risks of *L. pneumophila* exposure and infection.[17] Therefore, comprehensive understanding of *L. pneumophila* adhesion and detachment associated with biofilms will elucidate the factors affecting *L. pneumophila* transmission to humans and provide guidelines for *L. pneumophila* risk control in DWDS.

Chemical (e.g., solution ionic strength) and physical (e.g., biofilm roughness and flow conditions in DWDS) factors may control adhesion and detachment of *L. pneumophila* and other pathogens associated with biofilms. Increasing ionic strength was believed to control bacteria adhesion on a variety of surfaces (Teflon, glass, protein coated glass, and other surfaces) through reducing the electrostatic repulsion between bacteria and the surface.[18–21] However, on single or multispecies biofilms, ionic strength was found to have little to no effect on adhesion of *E. coli* and *Erwinia chrysanthemi*,[22,23] indicating that electrostatic interactions did not control adhesion on biofilms. Thus, the effects of physical factors on bacteria adhesion on biofilms should be studied, but were addressed in only limited studies. For example, unevenness of a surface, which is referred to as surface roughness, was found to influence *E. coli* adhesion on *Pseudomonas aeruginosa* biofilms[24] and multispecies biofilms.[23] However, mechanisms of how biofilm roughness affects *L. pneumophila* and other bacteria adhesion and if biofilm roughness affects bacteria detachment were unknown. In addition to biofilm roughness, hydrodynamic conditions were also shown to influence cell adhesion to and detachment from multiple surfaces.[25–28] High shear stress caused by high flow velocity prevented cell adhesion onto the clean and smooth surfaces,[25,27] and enhanced detachment of the adhered biomass.[25,28,29] Nevertheless, for heterogeneous rough biofilm surfaces, local hydrodynamics could be disturbed by the surface asperities. This local hydrodynamics created by surface asperities may alter the adhesion and detachment of *L. pneumophila* and other bacteria associated with biofilms and should be investigated. However, previous studies on *L. pneumophila* adhesion and detachment did not address the effect of biofilm physical properties nor hydrodynamics conditions.[30,31] Therefore, a comprehensive study identifying the combined effect of surface roughness and

hydrodynamics on *L. pneumophila* adhesion and detachment is needed to understand *L. pneumophila* transmission in DWDS.

To fill the aforementioned research gaps, we determined the physical structure of groundwater biofilms under different flow conditions and the influence of these structures on the mechanisms of *L. pneumophila* adhesion and detachment. Specifically, we (1) used optical coherence tomography (OCT) to determine whether the biofilm deform when being exposed to flow with velocity up to 0.7 m/s; (2) experimentally quantified *L. pneumophila* adhesion on biofilms under low flow conditions and used computational fluid dynamics (CFD) to reveal the role of hydrodynamics created by surface roughness; and (3) identified the effect of biofilm roughness and hydrodynamics on detachment of preadhered *L. pneumophila*. This study sheds light on the mechanism affecting *L. pneumophila* adhesion to and detachment from biofilms, which are likely key steps in the transmission of the legionellosis disease from DWDS.

MATERIALS AND METHODS

Biofilm Preparation

A local groundwater source, which is also a source for drinking water in Urbana–Champaign, IL, was selected for growing biofilms in this study. The microbial communities from the groundwater and the time required for biofilm development have been previously characterized.[23,32] PVC coupons (RD 128-PVC, BioSurface Technologies Corporation, Bozeman, MT) with the diameter of 1.26 cm were selected as the substratum of biofilm because PVC is a common plastic material used for drinking water pipes. Biofilms were grown on PVC coupons in CDC reactors (CBR 90-2, BioSurface Technologies Corporation, Bozeman, MT) with continuous stirring at 125 rpm or Re of 2384, as previously described.[23]

L. pneumophila Cell Preparation

L. pneumophila (ATCC 33152) tagged with green fluorescence protein (GFP) by electroporating plasmids pBG307 was used in this study.[33] *L. pneumophila* cells were grown in buffered yeast extract medium, harvested, and resuspended in potassium chloride (KCl) solutions for subsequent adhesion experiments. More details of *L. pneumophila* culturing and characterizing are documented in the Supporting Information (SI).

Adhesion Experiment and Sherwood Number Calculation

Adhesion experiments of GPF-tagged *L. pneumophila* cells on unstained 2-, 4-, 8-, 14-, and 29-week biofilms and PVC surfaces were conducted using a parallel plate flow chamber (FC 71, BioSurface Technologies Corporation, MT). During each experiment, electrolyte solution with 1–5 × 10^7 cells/mL of *L. pneumophila* was pumped into the flow chamber at an average flow velocity of 0.007 m/s with Re of 1.26 for 30 min. This average flow

ASSOCIATED CONTENT

Supporting Information

Details on the methodology, Figures S1–S5, and Tables S1– S7. This material is available free of charge via the Internet at http://pubs.acs.org/.

velocity was kept constant for all experiments to simulate near stagnant laminar flow conditions in a DWDS, when the highest adhesion of planktonic bacteria to solid surface is expected.[25,34] Measurements over DWDS in Ohio and Arizona found up to 35% and 16% of the total pipe carrying water in laminar flow region, respectively.[35,36] Ionic strengths ranging from 3 to 300 mM were selected to determine the role of electrostatic interactions on adhesion. The number of *L. pneumophila* cells adhering to biofilms was determined with the aid of a fluorescence microscope or a confocal laser-scanning microscope (CLSM). For experiments using the fluorescence microscope (Leica DM15000 M), the images of the biofilm surface with adhered cells were taken at 1 min intervals throughout the 30 min. adhesion experiments, and the number of adhered cells was counted from each image. For each combination of biofilm age and ionic strength, adhesion experiments were conducted with three biofilms. The imaging area of 0.395 × 0.296 mm^2 in the center of each biofilm coupon was chosen. For experiments with CLSM (TCS SP2 RBB, Leica Microsystems), real-time determination of adhered cells was not possible because this method requires time to scan the biofilm at different depths. Instead, the three-dimensional image of adhered cells through the whole biofilm body was obtained. The number of total adhered cells after 30 min. of adhesion process was determined by the 3-D image.

The adhesion was expressed as Sherwood numbers, which represent the average local particle transfer rate to the collector surface.[37–40] The Sherwood number was calculated as the ratio of experimentally determined cell adhesion mass transfer divided by diffusive mass transfer of the cells, and used to present adhesion data so that the data set obtained could be compared with previous work.[37–41] More details of the flow chamber dimension, adhesion experiments and the Sherwood number calculation were described in the SI.

Detachment Experiment

The detachment of preadhered *L. pneumophila* from a relatively smooth biofilm and rough biofilm with the relative roughness coefficient of 0.17 and 0.27, respectively, was determined for the average flow velocities of 0.1, 0.3, and 0.7 m/s. These flow velocities correspond to Re of 1.26, 50, and 126. The highest flow velocity was selected to match the design flow rate of 11.4 L/min (3 GPM) of some states in the United States and a common shower pipe size of 0.75 in. or 1.9 cm.[42,43] *L. pneumophila* cells were allowed to attach onto the biofilm surface for 30 min at 0.007 m/s, as described in the adhesion experiment. A 3 mM KCl solution free of *L. pneumophila* was then introduced into the flow chamber at 0.007 m/s to wash the flow chamber and remove *L. pneumophila* cells floating above the biofilm surface. After washing the flow chamber for 20 min, the average flow velocity was increased to promote the detachment of adhered *L. pneumophila* cells from biofilms. The detachment process under each flow condition during a period of 30 min was recorded using a fluorescence microscope at intervals of 1 min. The number of retained cells on biofilm surfaces at each imaging time point was counted. The ratio of retained cells (R_t), final detached cell ratio (D_{final}), and the time for 90% of maximal cell detachment (T_{90}) was determined and described in the SI.

OCT Image Collection and Structure Analysis for Biofilms

Optical coherence tomography (OCT) was used to determine the roughness and thickness of the different biofilms. For OCT measurements, the coupons were removed from the CDC reactors and placed in a flow chamber, which was also used for adhesion and detachment experiments. Biofilm images were captured by a spectral-domain OCT system, which utilized a mode-locked titanium:sapphire laser source (Kapteyn-Murnane Laboratories, Inc., Boulder, CO) centered at 800 nm with a 120 nm bandwidth. Axial and transverse imaging resolution was 1.8 and 16 μm. Two-dimensional cross-sectional images were acquired at a 25 Hz imaging rate with 1000 A-scans (columns) per image. Biofilm mean thickness, relative roughness coefficient, and biofilm surface enlargement coefficient[44] was obtained by analyzing 20–25 OCT images for a given biofilm with the program developed by Derlon et al.[45] and described in the SI.

As a control experiment to identify the possible biofilm structure deformation under the flow conditions used in the adhesion experiments, OCT images were taken for a selected mature biofilm when continuously exposed to different average flow velocities (0, 0.007, and 0.03 m/s) in the flow cell. For monitoring the possible biofilm structure change under high flow rate used in detachment experiments, both the 30- (rough) and 34-week (smooth) biofilms were continuously imaged by OCT for half an hour when the 3 mM KCl solution was introduced to the flow cell at the flow velocities of 0.1, 0.3, and 0.7 m/s. Each measurement was repeated three times on different biofilm coupons from the same reactor.

CFD and Particle Tracing Simulation for Flow Across the Biofilms

Ten rough (4-week, relative roughness coefficient = 0.76 ± 0.07) and ten smooth (14-week, relative roughness coefficient = 0.30 ± 0.07) biofilm 2-dimensional contours obtained from OCT imaging were used for the simulation of velocity distribution and particle movement above the biofilm surface in the flow chamber. The simulation was conducted with COMSOL Multiphysics 4.3a (Comsol Inc., Burlington, MA) and had two steps. For the first step, the Navier–Stokes equation for flow profiles inside the flow chamber was numerically solved with a no-slip boundary condition on both biofilm surfaces and the glass cover slide wall. The initial velocity was set as the average flow velocity (0.007 m/s) inside the flow cell. In the second simulation step, spherical particle movement in this flow field was simulated based on Newtonian's law of motion, drag force, and Brownian motion. Drag force was calculated from Stokes equation and flow velocity. Brownian motion was determined by particle size (2 μm), dynamic viscosity, and a random number generator factor for particle diffusion. 1000 particles were continuously delivered together with the fluid into the flow chamber for 10 s. These particles were dispersed in the flow by the drag force and Brownian motion. Finally, the adhesion of particles was represented by deposition probability, which was calculated by dividing the final number of adhered particles with the number of total released particles. The simulation was conducted in the fluid phase, and the flow was at steady state.

The Navier–Stokes equation was also solved numerically with no-slip boundary conditions for all average flow velocities (0.1, 0.3, and 0.7 m/s) used in detachment experiments for the selected rough and smooth biofilm OCT contours. Shear stress distribution, a critical factor

controlling the detachment of *L. pneumophila* from biofilm, was calculated based on these velocity profiles. This shear stress simulation was time-independent. More physical parameters used in particle tracing and shear stress simulation are in the SI (Table S5).

Statistical Analysis

Statistical analysis was conducted for all Sherwood numbers obtained from fluorescence microscope and CLSM adhesion experiments. The significance level of 0.05 was used for both one way ANOVA and *t* test. See the SI for more details.

RESULTS AND DISCUSSION

Biofilm Structure Determined by OCT Imaging

The effects of biofilm age on its thickness and roughness were determined under no flow conditions. The average biofilm thickness increased with age, from 20 ± 4 μm for a 4-week biofilm to 38 ± 5 μm for a 14-week biofilm. After 14 weeks, the biofilm thickness stabilized. Specifically, the average thickness between a 29-week biofilm (32 ± 14 μm) and a 14-week biofilm (38 ± 5 μm) was similar ($\alpha = 0.05$, $p = 0.22$). The highest relative roughness coefficient of 0.76 ± 0.07 was observed for the 4-week biofilm. The relative roughness coefficient decreased with the biofilm age to 0.30 ± 0.07 at 14-week. At the 29th week, the roughness increased to 0.67 ± 0.13. These biofilm thickness and roughness values are listed in SI Table S1. Overall, the change of biofilm roughness was not correlated with its thickness.

Possible biofilm deformation due to flow through the experimental chamber containing the biofilms was investigated under two flow regimes using OCT imaging. For the low flow conditions, when the flow velocity increased from 0 to 0.03 m/s, the biofilm contours at the same location did not show deformation (Figure 1). The average biofilm thickness and roughness at different locations under different flow velocities were statistically similar (SI Table S2). Therefore, the effect of biofilm structural change during the adhesion experiments and particle tracing simulation, which used a flow velocity of 0.007 m/s, was not considered.

For the high flow conditions, a relatively rough biofilm and a smooth biofilm with roughness coefficients of 0.27 and 0.17, respectively, were imaged by OCT during continuous exposure to the average flow velocities of 0.1, 0.3, and 0.7 m/s for half an hour. At all flow conditions used here and in the detachment experiment, OCT (with vertical resolution of 2.8 μm under flow condition) did not detect significant structural deformation for both 30- and 34-week biofilms. For example, the 30-week biofilm contours at the beginning and the end of detachment experiments under different average flow velocities are shown in Figure 2. After 30 min of exposure time to flow velocities of 0.1, 0.3, and 0.7 m/s, biofilms maintained their original structure. In addition, the average roughness and thickness of each biofilm before and after exposure to different flow velocities were statistically the same (SI Table S3). These observations that biofilm structure did not change during detachment experiments indicated that the biofilms grown from the groundwater were rigid enough to resist high shear stress caused by the high flow velocity. The rigid structure of

biofilms may be due to the long time used for biofilm development, the low nutrient, and the high hardness (1.63 mM Ca^{2+}) of the feed groundwater. Previous study also revealed a more rigid biofilm structure under reduced nutrient conditions.[46] Calcium ions in the feed groundwater may strengthen biofilms structure by cross-linking the biofilm matrix, allowing better resistance to shear stress.[47–49] Because the biofilms used in this study were resistant to a wide range of flow conditions (from 0 to 0.7 m/s), the effect of structural change during detachment experiments and flow simulation could be ignored.

Adhesion Experiments of *L. pneumophila* on Biofilms Grown on PVC Coupons

L. pneumophila adhesion on biofilms with different roughness was experimentally measured for solutions containing from 3 to 300 mM ionic strength to determine whether electrostatic double layer compression or biofilm surface roughness control the adhesion. *L. pneumophila* adhesion on PVC surfaces and 2-week biofilms increased with ionic strength (Figure 3a). This observation with fluorescent microscopy was consistent with lower electrostatic repulsion between PVC surface and *L. pneumophila* cells based on less negative electrophoretic mobility values of the cells at higher ionic strength. The electrophoretic mobility of *L. pneumophila* cells was −1.90 ± 0.09, −1.58 ± 0.10, and −0.52 ± 0.06 μm·V/(s·cm) (N = 12) at 3, 10, and 100 mM, respectively (SI Figure S2). At 300 mM, the adhesion on both PVC and the 2-week biofilm was lower than that at 100 mM. The observation that adhesion leveled off with further increases in ionic strength has already been reported for other colloidal particles.[19,33,50,51] In contrast to the observation that *L. pneumophila* adhesion on PVC and 2-week biofilm surfaces is dependent on ionic strength, we found that on those biofilms older than 4 weeks with thickness from 20 to 32 μm (SI Table S1), the Sherwood numbers for *L. pneumophila* were similar at ionic strengths from 3 to 300 mM (Figure 3a), indicating ionic strength did not control *L. pneumophila* adhesion on older biofilms. For example, on the 14-week biofilm, the Sherwood number values obtained at 3 mM, 10 mM, and 100 mM were statistically similar (t test, $\alpha = 0.05$, $p = 0.9$). *L. pneumophila* adhesion measured by CLSM was also independent of ionic strength (Figure 3b). In addition, Sherwood numbers obtained for the 14-week biofilm at 10 mM KCl using these two imaging methods were statistically similar ($p = 0.85$). The observation that CLSM imaging gave the same results as fluorescence microscopy suggested that, under these testing conditions, *L. pneumophila* adhered to the biofilm surface instead of penetrating into the biofilm matrix. The Sherwood numbers measured for all cases were less than one, varying from 0.003 ± 0.001 to 0.08 ± 0.03, in agreement with previously reported values of Sherwood numbers from 0.004 to 0.29 for *E. coli* adhesion on bare and zeolite-coated aluminum alloy and stainless steel surfaces in 10–100 mM KNO_3 solution.[41]

While the adhesion of *L. pneumophila* on older biofilms was independent of ionic strength, we found that the Sherwood numbers measured at both 3 and 100 mM correlated positively with the relative roughness coefficient (Figure 4 and SI FIgure S3). Specifically, with biofilm relative roughness coefficient increasing from 0.30 ± 0.07 (14-week biofilm) to 0.76 ± 0.07 (4-week biofilm), Sherwood numbers increased from 0.03 ± 0.01 to 0.07 ± 0.02 at 3 mM. This observed higher adhesion on rougher surfaces could be explained by an enlarged surface area due to the surface roughness as reported previously.[52] However, while the surface area enlargement parameter of the roughest biofilms was 1.5 times larger than that of

the smoothest biofilms (3.2 for 4-week biofilms vs 2.1 for 14-week biofilms), the adhesion of *L. pneumophila* on the roughest biofilms was twice larger than that on the smoothest biofilms. Thus, other factors besides the enlarged surface area contributed to the higher adhesion on rough surfaces.

Cell adhesion is controlled by surface interactions and hydrodynamics in flow conditions.[25,53] As observed here, the increase in ionic strength and reduction in electrostatic repulsion did not lead to higher adhesion on older biofilms. Previous study also reported that the local hydrodynamics near the surface overcome the repulsive DLVO interactions and make the roughness asperity act as attractive locations allowing the particles getting closer to the substrate surface.[54] Therefore, effects of hydrodynamics on *L. pneumophila* adhesion should be considered. To explain how local hydrodynamic conditions created by surface roughness influences adhesion of particles with similar size and density as *L. pneumophila* cells, we performed simulation of the flow above the biofilm surface and the movement of particles in the flow. This simplifying assumption will only allow an indirect and qualitative comparison of the experimental trend with simulation results.

Hydrodynamics and Particle Tracing Simulation for Low Flow Velocity Conditions Used in Adhesion Experiments

The simulation results for flow velocity distribution and particle tracing above selected rough (4-week) and smooth (14-week) biofilm contours exposed to an average flow velocity of 0.007 m/s were obtained to determine the role of surface roughness on particle deposition. As shown in Figure 5a,b, particles adhered more on the rough surface compared with that on the smooth surface. The average values of deposition probability on 10 rough and 10 smooth biofilm surfaces were 0.13 ± 0.03 and 0.06 ± 0.01, respectively. Statistically higher particle adhesion (*t* test, $p = 0.0002$) obtained for rough surfaces compared with smooth surfaces suggested that the surface roughness enhanced particle deposition. On the rough biofilm surface (Figure 5a), most of the particles accumulated near the peak and on the side of the asperity that was facing the flow. On the smooth surface (Figure 5b), however, adhered particles were distributed more randomly along the biofilm surface.

On the basis of the particle capture theory,[55] we propose that the direction change of streamline above the rough surface enhanced the interception of particles with the rough surface asperities, allowing additional particle adhesion. The distribution and shape of the streamline was highly dependent on the structure of the surface boundary. Specifically, along the rough surface, the direction of the velocity vectors changed significantly (Figure 5a). In contrast, along the smooth surface, the velocity vectors maintained their horizontal direction. When particles moved with the flow streamline and got closer to the asperity present on the rough surface, these particles could be directly blocked by this asperity or impact with this asperity by inertia (Figure 5c,d). This process was facilitated at the location where the streamline intercepted with roughness asperities or where flow direction changed dramatically, allowing more particles to accumulate at the peaks and the side of the asperity that was facing the flow. However, on the smooth surface, less particle interception was expected due to less variation of the streamline direction along the surface. Comparing the velocity distribution on both the rough and the smooth surfaces, a larger stagnant zone was

observed surrounding asperities on the rough surface versus the smooth surface. In these zones, particles could slowly move along the asperities, allowing enhanced interception between particles and roughness asperities. On a smooth surface, by contrast, there is a low probability of particle interception with surface roughness asperities. In summary, the higher particle adhesion on rougher surfaces appeared to be due to the enhanced interception resulting from the local hydrodynamic conditions created by surface roughness.

Qualitative Comparison of Experimental Results and Simulation Results

The results of *L. pneumophila* adhesion experiments show that *L. pneumophila* adhesion was enhanced on rougher biofilms. The simplified particle tracing simulation, for the first time, showed the detailed local flow profile and particle movement above complex biofilm profiles obtained by OCT. The simulation results revealed the enhanced particle interception on rough surfaces in agreement with the experimental results. While this simulation identified the roles of surface structure on adhesion, it may not exactly reflect the movement of *L. pneumophila* in a real flow system, such as DWDS, due to the following limitations. (1) Particles used in simulation were sphere shaped, while *L. pneumophila* cells are rod shaped. In our simulations, the micrometer scale difference was not considered due to the resolution of biofilm contours obtained from OCT technique. (2) For clearly showing the effect of surface roughness along the flow direction, we only conducted 2-D simulations above the cross-section profile of biofilms. 2-D simulations were commonly used in previous studies on hydrodynamics simulations for biofilms.[56,57] The possible particle diffusion and flow disturbances perpendicular to the main flow direction in 3-D space were not considered. (3) The simulation was conducted under a flow condition, including particle diffusion and convection. Under completely stagnant flow conditions in DWDS, particle diffusion will dominate the adhesion. Overall, although this simulation could not precisely represent the transport of *L. pneumophila* in real DWDS, it provided evidence of roughness enhancing particle adhesion by creating local hydrodynamics and supported the conclusions obtained from the adhesion experiments.

Detachment Experiments of *L. pneumophila* from Biofilms

Detachment of preadhered *L. pneumophila* from a selected rough biofilm and a smooth biofilm was experimentally determined at average flow velocities of 0.1, 0.3, and 0.7 m/s, which simulated the flow rate in DWDS. The ratios of cells retained on the biofilm to the total preadhered cells on the biofilm (R_t) as a function of time were determined. For both rough and smooth biofilms, R_t dropped rapidly with time, then became stable after a few minutes. For example, when the smooth biofilm was subjected to an average flow velocity of 0.1 m/s, R_t decreased from 1 to 0.42 in the first 6 min, then stopped decreasing over the next 24 min (SI Figure S4). The time required to achieve 90% of maximal cell detachment (T_{90}) and the final ratio of the total detached cells to total preadhered cells (D_{final}) for different flow conditions were calculated (SI Table S6). An increase in average flow velocity from 0.1 to 0.7 m/s led to higher detachment. For example, for the rough surface, D_{final} of 45%, 53%, and 73% were obtained under average flow velocities of 0.1, 0.3, and 0.7 m/s, respectively, indicating that more cells detached under the higher average flow velocity. In addition, T_{90} decreased from 9.8 to 3.3 min when the average flow velocity increased from 0.1 to 0.7 m/s, revealing a faster detachment of *L. pneumophila* under the

higher flow velocity. Higher shear stress caused by higher flow velocity was reported to lead to the increased cell detachment under increasing flow velocity.[25,34] Therefore, the observed dependence of *L. pneumophila* detachment with flow velocities was further explained using the simulation results of shear stress distribution in the flow chamber (SI Figure S5).

As evidenced from the OCT imaging and analysis, biofilms grown from groundwater used in this study had rigid structure resisting deformation when subjected to flow velocities up to 0.7 m/s. For this reason, biofilm deformation was not considered in the simulation for shear stress exerted by the water flow on the biofilm. According to the simulation results, when the average flow velocity increased from 0.1 to 0.7 m/s, the shear stress on both rough and smooth surfaces increased significantly. This increased shear stress with flow velocity has been shown to be responsible for the improved detachment rate of bacteria from glass surfaces.[25,34] In our study, the increased shear stress with increasing flow velocity also caused a 3 times faster *L. pneumophila* detachment from biofilms.

In addition to the observed detachment trend with flow velocity, detachment of *L. pneumophila* also depended on the biofilm roughness. Under the average flow velocities of 0.1 and 0.3 m/s, higher detachment was observed from smooth biofilm surface compared to rough biofilm surface. Under 0.3 m/s average flow velocity, T_{90} for the rough and smooth biofilm surface was 6.61 and 3.38 min, respectively, revealing a faster *L. pneumophila* detachment from the smooth biofilm surface. D_{final} of 53% and 74% were obtained for the rough and the smooth biofilm surface, indicating that larger amounts of preadhered cells were detached from the smooth biofilm surface. In contrast to the observation at lower flow velocities of 0.1 and 0.3 m/s, under an average flow velocity of 0.7 m/s, similar detachment of *L. pneumophila* from both rough and smooth biofilms was observed. Specifically, 73% and 77% of preadhered cells detached from the rough and the smooth biofilm surfaces at the end of detachment experiments, respectively.

Previous modeling study reported that larger hydrodynamic force would be required to detach particles from a rougher surface compared to a smooth surface.[58] Therefore, we compared the shear stress profiles exerted on the smooth and rough surfaces studied here. Compared with rough surface, the average flow velocities from 0.1 to 0.7 m/s exerted a more uniform shear stress distribution on the smooth surface. For example, under the average flow velocity of 0.3 m/s, on the rough surface (SI Figure S5b), the highest shear stress was formed near the peak of each asperity (cyan, yellow, and red areas with shear stress >6 Pa), while large low shear stress zones were formed underneath the peak (dark blue areas with shear stress <2 Pa). On the smooth surface (SI Figure S5e), shear stress on most of the area was >6 Pa. The larger low shear stress zones on the rough biofilm surface suggested that cells adhered in these zones were subjected to less shear stress penetration and therefore had a lower probability of detachment. On the smooth biofilm surface, however, the shear stress was distributed more uniformly, thus most of the biofilm surface was exposed to shear stress. Consequently, in contrast to the rough surface, more cells were expected to detach from the smooth biofilm surface. However, under the highest average flow velocity of 0.7 m/s used here, the high shear stress exerted on the biofilm may penetrate the biofilm causing detachment of biofilm surface layer, not just the preadhered

cells. For this reason, high shear stress caused the equally high detachment of *L. pneumophila* from both smooth and rough biofilm surfaces.

In summary, this study identified that *L. pneumophila* adhesion was enhanced by biofilm roughness because of the increased interception between the flowing particles and the surface on rough biofilms. After *L. pneumophila* adhered to the biofilm, subsequent cell detachment was facilitated by high average flow velocity. Biofilm roughness could protect *L. pneumophila* from detachment by creating larger low shear stress zones. A summary of the study results is provided in SI Table S7. These findings are relevant for pathogen control within premise plumbing. However, the *L. pneumophila* long-term colonization and release should be evaluated to shed light upon the fate and transport of pathogenic *L. pneumophila* in DWDS. The effect of practical conditions (e.g., temperature) and drinking water components (hardness, disinfectant, the presence of amoeba) need further investigation.

ACKNOWLEDGMENTS

This study was supported by EPA STAR grant R834870 to T.H.N. and W.T.L., and NIH R01 EB013723 to S.A.B. and G.L.M. We acknowledge Dr. Lu (Sun Yat-sen University) for the GFP plasmid, and Professors Picioreanu and van Loosdrecht (Delft University) for COMSOL.

REFERENCES

1. September SM, Els FA, Venter SN, Brozel VS. Prevalence of bacterial pathogens in biofilms of drinking water distribution systems. J. Water Health. 2007; 5(2):219–227. [PubMed: 17674571]
2. Declerck P. Biofilms: the environmental playground of *Legionella pneumophila*. Environ. Microbiol. 2010; 12(3):557–566. [PubMed: 19678829]
3. Lau H, Ashbolt N. The role of biofilms and protozoa in *Legionella* pathogenesis: implications for drinking water. J. Appl. Microbiol. 2009; 107(2):368–378. [PubMed: 19302312]
4. Thomas JM, Thomas T, Stuetz R, Ashbolt NJ. Your garden hose: a potential health risk due to *Legionella* spp. growth facilitated by free-living amoebae. Environ. Sci. Technol. 2014; 48(17): 10456–10464. [PubMed: 25075763]
5. Tison D, Pope D, Cherry W, Fliermans C. Growth of *Legionella pneumophila* in association with blue-green algae (cyanobacteria). Appl. Environ. Microbiol. 1980; 39(2):456–459. [PubMed: 6769388]
6. Wadowsky RM, Yee RB. Satellite growth of *Legionella pneumophila* with an environmental isolate of *Flavobacterium breva*. Appl. Environ. Microbiol. 1983; 46(6):1447–1449. [PubMed: 6660882]
7. Stout JE, Yu VL, Best MG. Ecology of *Legionella pneumophila* within water distribution systems. Appl. Environ. Microbiol. 1985; 49(1):221–228. [PubMed: 3977311]
8. Temmerman R, Vervaeren H, Noseda B, Boon N, Verstraete W. Necrotrophic growth of *Legionella pneumophila*. Appl. Environ. Microbiol. 2006; 72(6):4323–4328. [PubMed: 16751547]
9. Thomas JM, Ashbolt NJ. Do free-living amoebae in treated drinking water systems present an emerging health risk? Environ. Sci. Technol. 2010; 45(3):860–869. [PubMed: 21194220]
10. Cargill KL, Pyle BH, Sauer RL, McFeters GA. Effects of culture conditions and biofilm formation on the iodine susceptibility of *Legionella pneumophila*. Can. J. Microbiol. 1992; 38(5):423–429. [PubMed: 1643585]
11. Cooper IR, Hanlon GW. Resistance of *Legionella pneumophila* serotype 1 biofilms to chlorine-based disinfection. J. Hosp. Infect. 2010; 74(2):152–159. [PubMed: 19783074]
12. Donları, R.; Murga, R.; Carpenter, J.; Brown, E.; Besser, R.; Fieids, B. Monochloramine disinfection of biofilm-associated *Legionella pneumophila* in a potable water model system. In: Marre, R., editor. Legionella. Novelty, OH: ASM Press; 2002.
13. Cianciotto NP. Pathogenicity of *Legionella pneumophila*. Int. J. Med. Microbiol. 2001; 291(5): 331–343. [PubMed: 11727817]

14. Adams D, Jajosky R, Ajani U, Kriseman J, Sharp P, Onwen D, Schley A, Anderson W, Grigoryan A, Aranas A. Summary of notifiable diseases—United States, 2012. MMWR. Morbidity and Mortality Weekly Report. 2014; 61(53):1–121. [PubMed: 25233134]
15. Hicks, LA.; Garrison, LE.; Nelson, GE.; Hampton, LM. Legionellosis — United States, 2000–2009. Office of Surveillance, Epidemiology, and Laboratory Services, Centers for Disease Control and Prevention (CDC), U.S. Department of Health and Human Services; 2011 Aug 19. p. 1083-1086.
16. de Jong, B.; Coulombier, D.; Hallström, LP.; Takkinen, J.; Ursut, D.; Zucs, P. Legionnaires disease in Europe 2012. European Centre for Disease Prevention and Control, ECDP; 2014.
17. Schoen ME, Ashbolt NJ. An in-premise model for *Legionella* exposure during showering events. Water Res. 2011; 45(18):5826–5836. [PubMed: 21924754]
18. Abbott A, Rutter P, Berkeley R. The influence of ionic strength, pH and a protein layer on the interaction between Streptococcus mutans and glass surfaces. J. Gen. Microbiol. 1983; 129(2): 439–445. [PubMed: 6842181]
19. Walker SL, Redman JA, Elimelech M. Influence of growth phase on bacterial deposition: Interaction mechanisms in packed-bed column and radial stagnation point flow systems. Environ. Sci. Technol. 2005; 39(17):6405–6411. [PubMed: 16190193]
20. Rijnaarts HHM, Norde W, Lyklema J, Zehnder AJB. DLVO and steric contributions to bacterial deposition in media of different ionic strengths. Colloid Surf., B. 1999; 14(1–4):179–195.
21. Long G, Zhu P, Shen Y, Tong M. Influence of extracellular polymeric substances (EPS) on deposition kinetics of bacteria. Environ. Sci. Technol. 2009; 43(7):2308–2314. [PubMed: 19452879]
22. Liu Y, Yang C-H, Li J. Adhesion and retention of a bacterial phytopathogen *Erwinia chrysanthemi* in biofilm-coated porous media. Environ. Sci. Technol. 2007; 42(1):159–165. [PubMed: 18350891]
23. Janjaroen D, Ling FQ, Monroy G, Derlon N, Morgenroth E, Boppart SA, Liu WT, Nguyen TH. Roles of ionic strength and biofilm roughness on adhesion kinetics of *Escherichia coli* onto groundwater biofilm grown on PVC surfaces. Water Res. 2013; 47(7):2531–2542. [PubMed: 23497979]
24. Wu M-Y, Sendamangalam V, Xue Z, Seo Y. The influence of biofilm structure and total interaction energy on *Escherichia coli* retention by *Pseudomonas aeruginosa* biofilm. Biofouling. 2012; 28(10):1119–1128. [PubMed: 23075008]
25. Boks NP, Norde W, van der Mei HC, Busscher HJ. Forces involved in bacterial adhesion to hydrophilic and hydrophobic surfaces. Microbiology. 2008; 154(10):3122–3133. [PubMed: 18832318]
26. Christersson CE, Glantz PO, Baier RE. Role of temperature and shear forces on microbial detachment. Scand J. Dent Res. 1988; 96(2):91–98. [PubMed: 3162604]
27. Raya A, Sodagari M, Pinzon NM, He X, Newby BMZ, Ju LK. Effects of rhamnolipids and shear on initial attachment of *Pseudomonas aeruginosa* PAO1 in glass flow chambers. Environ. Sci. Pollut. Res. 2010; 17(9):1529–1538.
28. Rittman BE. The effect of shear stress on biofilm loss rate. Biotechnol. Bioeng. 1982; 24(2):501–506. [PubMed: 18546318]
29. Horn H, Reiff H, Morgenroth E. Simulation of growth and detachment in biofilm systems under defined hydrodynamic conditions. Biotechnol. Bioeng. 2003; 81(5):607–617. [PubMed: 12514810]
30. Stewart CR, Muthye V, Cianciotto NP. *Legionella pneumophila* persists within biofilms formed by *Klebsiella pneumoniae*, *Flavobacterium* sp., *Pseudomonas* sp under dynamic flow conditions. PLoS One. 2012; 7(11):e50560. [PubMed: 23185637]
31. Mampel J, Spirig T, Weber SS, Haagensen JAJ, Molin S, Hilbi H. Planktonic replication is essential for biofilm formation by *Legionella pneumophila* in a complex medium under static and dynamic flow conditions. Appl. Environ. Microbiol. 2006; 72(4):2885–2895. [PubMed: 16597995]
32. Ling F, Liu WT. Impact of chloramination on the development of laboratory-grown biofilms fed with filter-pretreated groundwater. Microbes Environ. 2013; 28(1):50–57. [PubMed: 23124766]

33. Chen DQ, Zheng XC, Lu YJ. Identification and characterization of novel ColE1-type, high-copy number plasmid mutants in *Legionella pneumophila*. Plasmid. 2006; 56(3):167–178. [PubMed: 16828158]
34. McClaine JW, Ford RM. Characterizing the adhesion of motile and nonmotile *Escherichia coli* to a glass surface using a parallel-plate flow chamber. Biotechnol. Bioeng. 2002; 78(2):179–189. [PubMed: 11870609]
35. Buchberger, S.; Carter, J.; Lee, Y.; Schade, T. Random Demands, Travel Times, and Water Quality in Deadends. Denver, CO: AwwaRF; 2003.
36. Romero-Gomez P, Choi CY. Axial dispersion coefficients in laminar flows of water-distribution systems. J. Hydraul. Div., Am. Soc. Civ. Eng. 2011; 137(11):1500–1508.
37. Darbha GK, Fischer C, Luetzenkirchen J, Schäfer T. Site-specific retention of colloids at rough rock surfaces. Environ. Sci. Technol. 2012; 46(17):9378–9387. [PubMed: 22861645]
38. Darbha GK, Schäfer T, Heberling F, Lüttge A, Fischer C. Retention of latex colloids on calcite as a function of surface roughness and topography. Langmuir. 2010; 26(7):4743–4752. [PubMed: 20201604]
39. Kline TR, Chen G, Walker SL. Colloidal deposition on remotely controlled charged micropatterned surfaces in a parallel-plate flow chamber. Langmuir. 2008; 24(17):9381–9385. [PubMed: 18656970]
40. Song L, Elimelech M. Particle deposition onto a permeable surface in laminar flow. J. Colloid Interface Sci. 1995; 173(1):165–180.
41. Chen G, Beving DE, Bedi RS, Yan YS, Walker SL. Initial bacterial deposition on bare and zeolite-coated aluminum alloy and stainless steel. Langmuir. 2009; 25(3):1620–1626. [PubMed: 19123799]
42. [05/10/2014] Ohio Administrative Code: Chapter 4101 Water Supply systems. http://codes.ohio.gov/oac/
43. Virginia Plumbing Code: Chapter 6 Water supply and distribution. https://www2.iccsafe.org/states/Virginia/Plumbing/Plumbing_Frameset.html.
44. Picioreanu C, Van Loosdrecht MC, Heijnen JJ. Mathematical modeling of biofilm structure with a hybrid differential-discrete cellular automaton approach. Biotechnol. Bioeng. 1998; 58(1):101–116. [PubMed: 10099266]
45. Derlon N, Peter-Varbanets M, Pronk W, Morgenroth E. Predation influences the structure of biofilm developed on ultra-filtration membranes. Water Res. 2012; 46(10):3323–3333. [PubMed: 22534121]
46. Reipa V, Almeida J, Cole KD. Long-term monitoring of biofilm growth and disinfection using a quartz crystal microbalance and reflectance measurements. J. Microbiol. Methods. 2006; 66(3): 449–459. [PubMed: 16580080]
47. Huang J, Pinder K. Effects of calcium on development of anaerobic acidogenic biofilms. Biotechnol. Bioeng. 1995; 45(3):212–218. [PubMed: 18623140]
48. Harvey M, Forsberg CW, Beveridge TJ, Pos J, Ogilvie JR. Methanogenic activity and structural characteristics of the microbial biofilm on a needle-punched polyester support. Appl. Environ. Microbiol. 1984; 48(3):633–638. [PubMed: 16346629]
49. Chen X, Stewart P. Role of electrostatic interactions in cohesion of bacterial biofilms. Appl. Microbiol. Biotechnol. 2002; 59(6):718–720. [PubMed: 12226730]
50. Liu Y, Janjaroen D, Kuhlenschmidt MS, Kuhlenschmidt TB, Nguyen TH. Deposition of *Cryptosporidium parvum* oocysts on natural organic matter surfaces: microscopic evidence for secondary minimum deposition in a radial stagnation point flow cell. Langmuir. 2009; 25(3): 1594–1605. [PubMed: 19133757]
51. Yuan B, Pham M, Nguyen TH. Deposition kinetics of bacteriophage MS2 on a silica surface coated with natural organic matter in a radial stagnation point flow cell. Environ. Sci. Technol. 2008; 42(20):7628–7633. [PubMed: 18983085]
52. Webster TJ, Siegel RW, Bizios R. Osteoblast adhesion on nanophase ceramics. Biomaterials. 1999; 20(13):1221–1227. [PubMed: 10395391]

53. Kalasin S, Dabkowski J, Nüsslein K, Santore MM. The role of nano-scale heterogeneous electrostatic interactions in initial bacterial adhesion from flow: A case study with *Staphylococcus aureus*. Colloids Surf., B. 2010; 76(2):489–495.

54. Kemps JA, Bhattacharjee S. Particle tracking model for colloid transport near planar surfaces covered with spherical asperities. Langmuir. 2009; 25(12):6887–6897. [PubMed: 19505160]

55. Spielman LA. Particle capture from low-speed laminar flows. Annu. Rev. Fluid Mech. 1977; 9(1): 297–319.

56. Picioreanu C, van Loosdrecht MC, Heijnen JJ. Two-dimensional model of biofilm detachment caused by internal stress from liquid flow. Biotechnol. Bioeng. 2001; 72(2):205–218. [PubMed: 11114658]

57. Zhang T, Cogan N, Wang Q. Phase field models for biofilms. II. 2-D numerical simulations of biofilm-flow interaction. Commun. Comput. Phys. 2008; 4(1):72–101.

58. Das SK, Schechter RS, Sharma MM. The role of surface roughness and contact deformation on the hydrodynamic detachment of particles from surfaces. J. Colloid Interface Sci. 1994; 164(1):63–77.

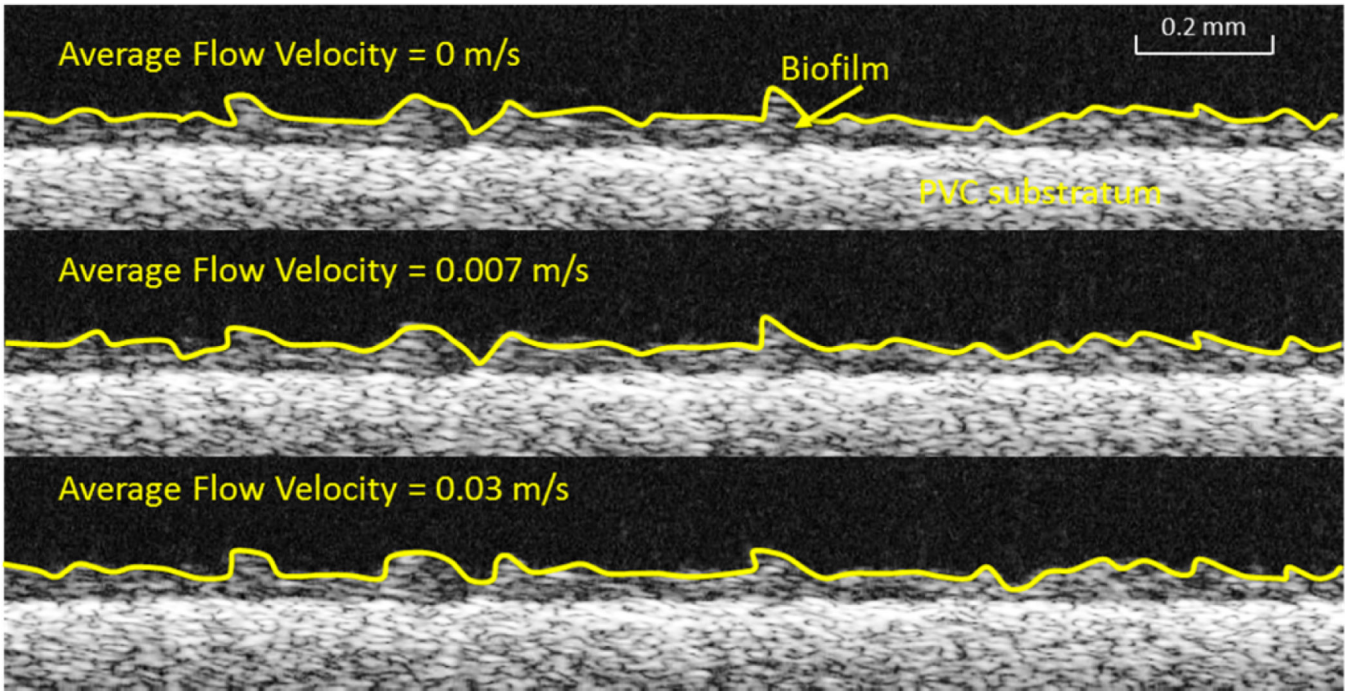

Figure 1.

OCT image of 8-week biofilm sequentially exposed to the average flow velocity of 0, 0.007, and 0.03 m/s. The yellow line is drawn manually and shows the boundary between the biofilm and water. These images were taken at the same location on biofilms when the biofilms were subjected to the flow with increasing velocity from 0 to 0.03 m/s.

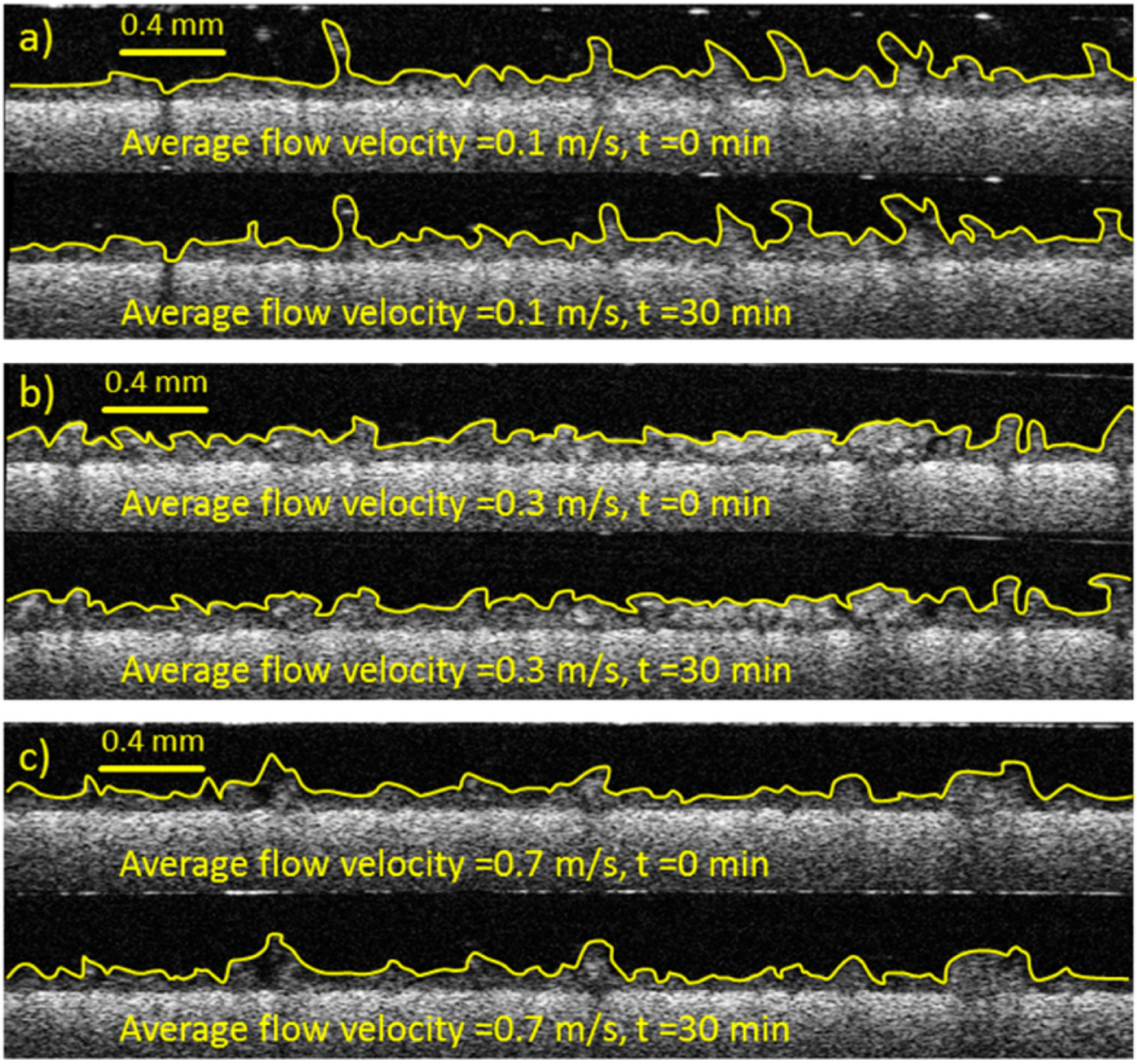

Figure 2.

OCT images of 30-week biofilms under the average flow velocity of (a) 0.1, (b) 0.3, and (c) 0.7 m/s. The yellow line is drawn manually and shows the boundary between the biofilm and water. All these images were captured when the biofilms were exposed to continuous flow with corresponding velocity. The flow exposing time was 30 min, and biofilms were imaged at the interval of 1 min. The images of these biofilms under flow taken at 1st min and 30th min were shown here.

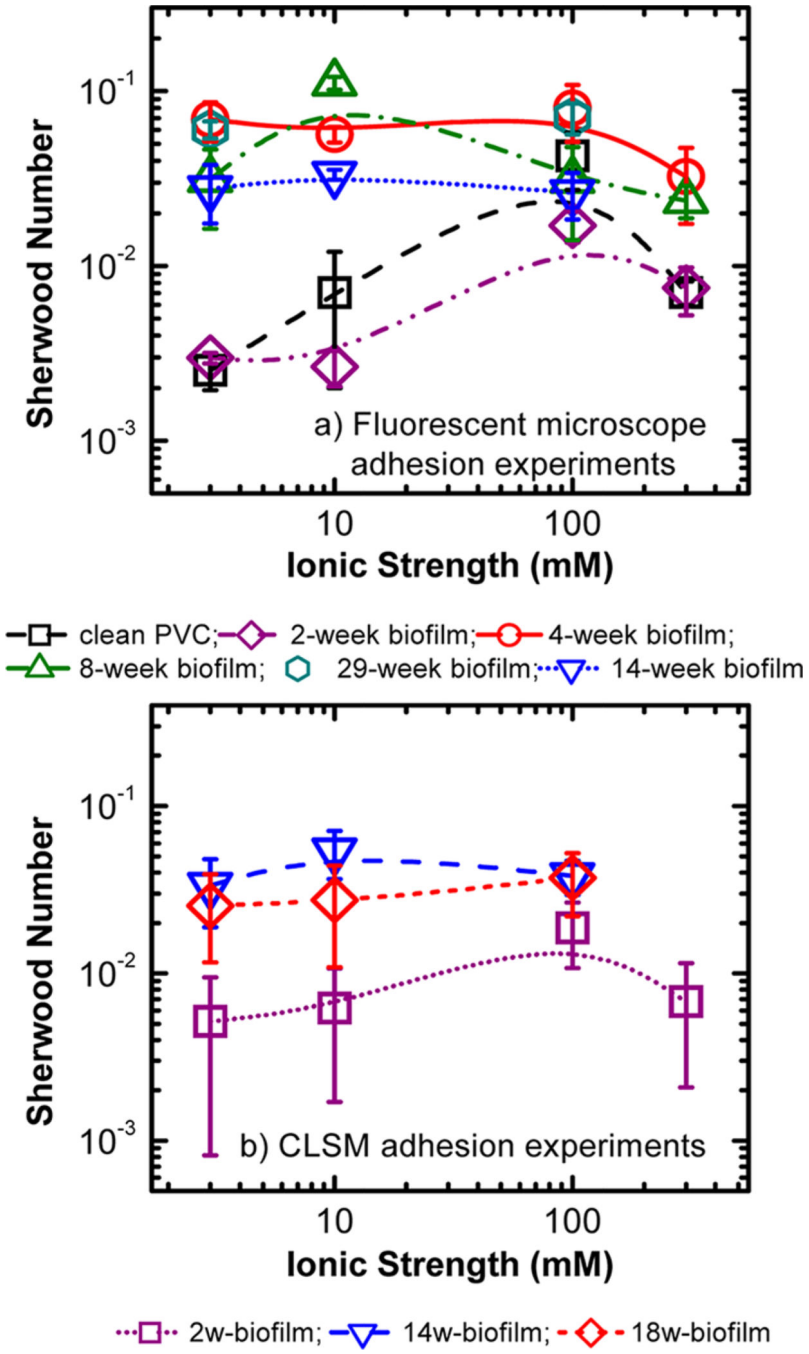

Figure 3.

Sherwood numbers of *L. pneumophila* deposited on PVC and biofilm surfaces grown at different times as a function of ionic strength (KCl) examined in (a) fluorescence microscope adhesion experiments and in (b) CLSM adhesion experiments at pH 8.2–8.5 and at 25 °C. Adhered cells and deposited cells were quantified by fluorescence microscopy and CLSM, respectively.

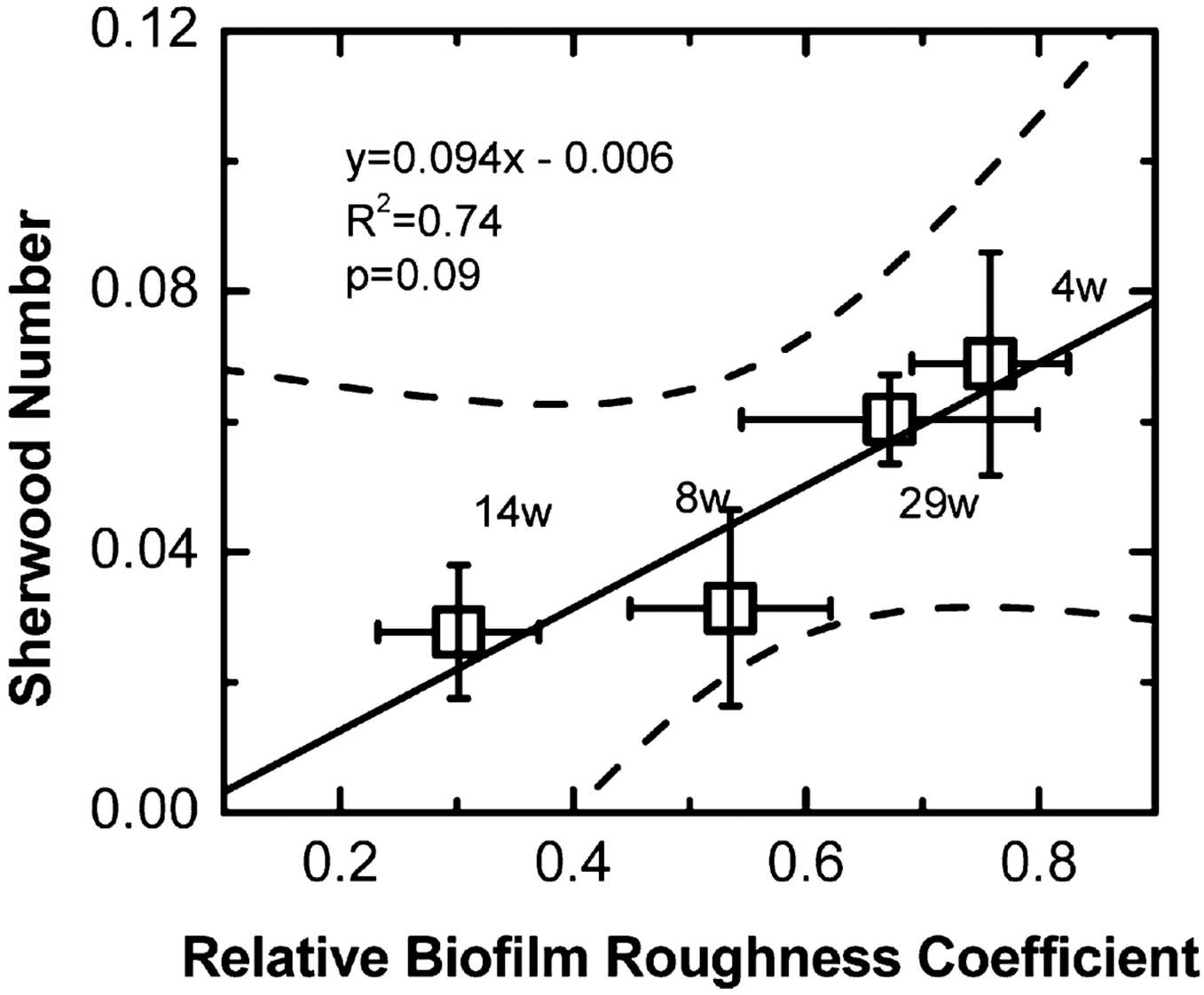

Figure 4.
Sherwood numbers of *L. pneumophila* examined in fluorescence microscope adhesion experiments as a function of relative biofilm roughness coefficient at 3 mM.

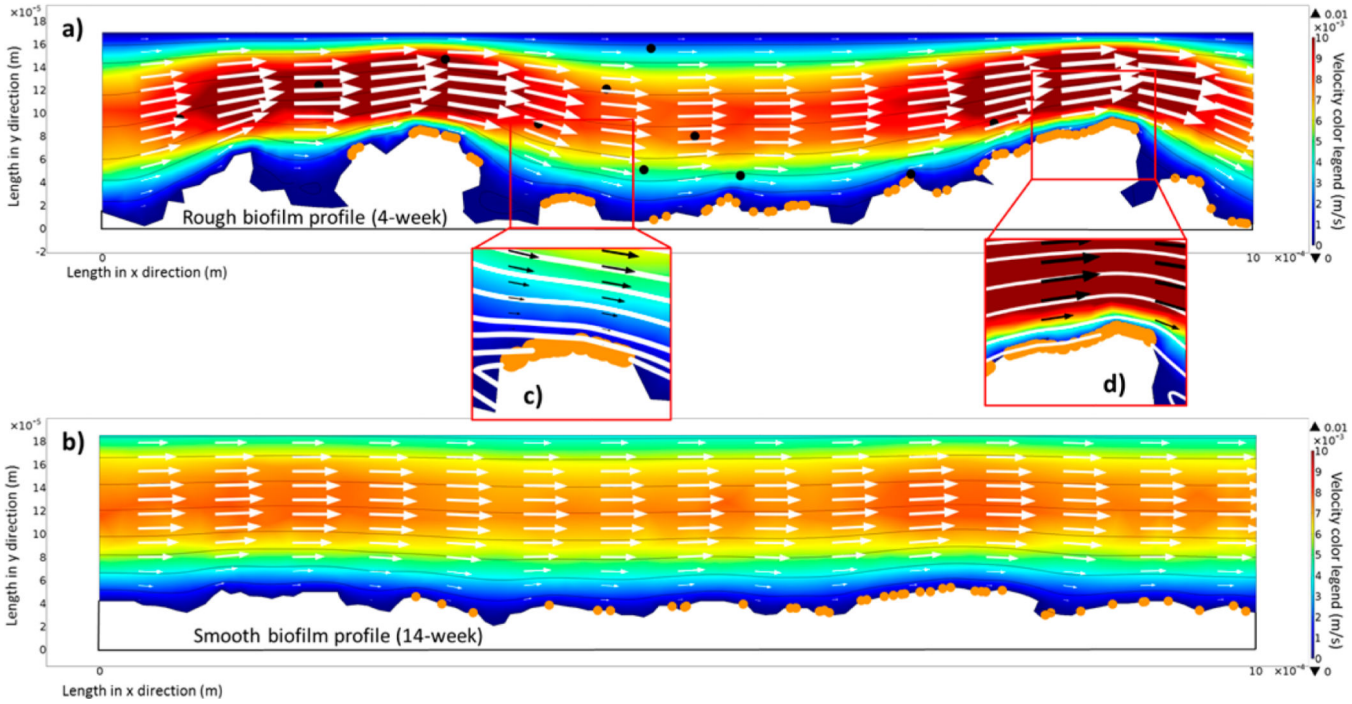

Figure 5.

Particle tracing simulation for (a) a rough 4-week biofilm and (b) a smooth 14-week biofilm at an average flow velocity of 0.007 m/s. (c) Particles accumulated in the peak of one of the asperities in rough biofilm. (d) Particles accumulated in the peak and the side facing flow in one aspertity in rough biofilm. Particle size is not drawn to scale. The horizontal length is 1 mm.